Symbiosis (2024) 92:91–109
https://doi.org/10.1007/s13199-023-00960-6

ORIGINAL PAPERS

Morpho-anatomical attributes of the Egyptian *Conocarpus erectus* L. (Combretaceae R.Br.) with its phytochemicals and fungal-endophytes

Nagwa R. A. Hussein[1] · **Eman G. A. M. El-Dawy**[1,2]

Received: 26 October 2022 / Accepted: 17 November 2023 / Published online: 21 December 2023

Abstract
Egyptian *Conocarpus erectus* L., or the buttonwood, was studied in different terms. This study used light and scanning electron microscopy, HPLC, and GC–MS analyses. Foliar morphology, anatomy of stems and leaves, pollen morphology, and phytochemical and endofungal attributes were investigated. It was an evergreen shrub with alternate leaves, a pair of nectary glands on the leaf base, and a few indumentums. Trichomes of both non- and glandular hairs were found. Stomata were sized, reaching 37.5 × 25.0 µm. They appeared on both abaxial and adaxial surfaces. The stem and leaf interior structure was typically like most dicots. Their internal structure revealed the mycelium of *Aspergillus flavus* throughout. Similarly, the accumulation of phenolic compounds as colored particles and integrated phytochemicals in crystalloid druses are observed internally. The endophytic fungus *A. flavus*, isolated from the leaves of *C. erectus*, contained the highest concentration of kojic acid. As a result, we could consider this *A. flavus* strain as a source of kojic acid for application in industry. Fungal and *C. erectus* extracts showed broad-range antifungal activity against three opportunistic human pathogenic fungi (*Geotrichum candidum* OL960606, *Neoscytalidium dimidiatum* OL960610, and *Scopulariopsis coprophila* OL960621). The major bioactive compounds of *C. erectus* leaf extracts were gallic acid, rutin, and rosmarinic acid. In conclusion, the endophytic *A. flavus* isolated from *C. erectus* has a variety of biological and medicinal uses that make it a potential commercial resource.

Keywords Anatomy · Foliar morphology · Phenolic compounds · Endophytic fungi · Antimicrobial

1 Introduction

Conocarpus erectus L. belongs to the family Combretaceae R.Br. (Bashir et al. 2015). It is an evergreen shrub known as buttonwood or button mangrove because its fruits resemble buttons. It frequently develops and spreads quickly in environments with poor soil fertility, elevated temperatures, poor drainage, and high saline levels (Gilman and Watson 1993; Nelson 1996; El-Mahrouk et al. 2010).

According to Stace (2007), *Conocarpus* is a genus that can be found in West Africa and both the East and West coasts of America, in addition to the non-mangrove member of the genus (*C. lancifolius*) that is found in northeast Africa and Arabia. Its hardwood is used in manufacturing furniture, fire, and charcoal (Al-Wabel et al. 2015). In the West Indies, *Conocarpus* is highly valuable for fuel (Stace 2007). The species *erectus* lives on Earth in tropical and subtropical locations (Schoener 1988; Rosa Galdino Bandeira 2003; Abdel-Hameed et al. 2012). However, *C. erectus* does start to have some ecological and environmental relevance. It might rebuild dunes, provide food and refuge for various species, protect the soil from storm damage, and restore dunes (Popp et al. 1989).

Conocarpus erectus's general vegetative features and internal structure are rarely discussed in the literature. Stace (2007) presented a proper identification based on its habits, distribution, morphology, palynology, and other features. Recently, the structure of pollen grains in *C. erectus* has been studied by Namjoyan et al. (2020). Earlier, Bailey (1976) described *C. erectus* as an evergreen tree up to 6 m high with a spreading crown, grey or brown bark, medium-green leaves, and greenish flowers in dense cone-like heads in terminal panicles. El-Mahrouk et al. (2010) studied the standard internal structure of the leaves and stem of *C. erectus* in comparison with irrigation with diluted seawater.

✉ Nagwa R. A. Hussein
nagwa_hussein@sci.svu.edu.eg

[1] Botany and Microbiology Department, Faculty of Science, South Valley University, Qena, Egypt

[2] Applied and Environmental Microbiology Center, South Valley University, Qena, Egypt

However, crucial taxonomic and characterization data can be obtained from the macro- and micro-morphological features of the plant's vegetative or reproductive parts. According to Afifi et al. (2021), *Conocarpus* is a genus of evergreen trees endemic to several habitats and tolerant of salt, heat, and drought. The results of that study demonstrated the production of polyphenol compounds by various plant parts of *C. erectus* and *C. lancifolius*. They also highlighted the unusual source of *Conocarpus* species for bioactive substances that can be utilized for pharmacological indications and the production of functional food. *Conocarpus* spp. found to include vanillic acid, p-coumaric acid, quercetin, rutin hydrate, flavone, t-ferulic acid, sinapic acid, and protocatechuic acid.

Aziz et al. (2018) showed that medicinal plants are functional food and medicine sources, especially in underdeveloped areas. Ali (2018) noted the presence of many natural plant compounds in *C. erectus* L. Polyphenols, including flavonoids and tannins, can be found. According to Koche et al. (2016), phenolics are a class of natural compounds with significant implications for medical practice. The antioxidant, anticancer, cytotoxic, antibacterial, and vasodilatory properties of phenolics are well documented. High hepatoprotective, antioxidant, and anticancer activity were observed in *C. erectus* (Shohayeb et al. 2013). This plant has also been found to have variable pharmacologically active phytochemicals, e.g., conocarpan, conocarpol, gallic acid, ellagic acid, ellagitannin, castalagin, quercetin, myricetin, syringetin, etc. (Sabi-ur-Rehman et al. 2019). This plant may have a significant role in preventing and curating diseases for which oxidants or free radicals are responsible (Abdel-Hameed et al. 2013).

Traditionally, people can use it for treating some disorders such as orchitis, prickly heat, headache, anemia, bleeding, catarrh, diabetes, diarrhea, conjunctivitis, tumors, gonorrhea, syphilis, and as an antipyretic and anti-inflammatory in the treatment of fever and swellings (Nascimento et al. 2016; Raza et al. 2016, 2018). Its bark and fruits manage diabetes, hemorrhoids, and wounds (Santos et al. 2018). The WHO revealed that various drugs are best obtained from medicinal plants.

Endophytic fungi, often known as plant-associated fungi, are a diverse group of microorganisms typically found asymptomatically in plant tissues or intercellular gaps. Some authors used different microscopy techniques to illustrate the occurrence of endofungi within the histological or anatomical structure of host plants (Salgado et al. 2007; Bernardi-Wenzel et al. 2010). Endophytes assist plants with several physiological processes, such as growth, reproduction, senescence, and others (Wilson 1995). Since endophytes live within the host plant, it is believed that they help the host plant respond to biotic and abiotic stress by increasing the host plant's tolerance to things like drought, salt, low temperatures, etc. (Arachevaleta et al. 1989; Wen et al. 2022). As a result of the mutualistic co-evolution of plants and their endophytes, several complex biological substances known as secondary metabolites have been produced. Endophytes may be used as alternative sources for these metabolites because several of them have been found to produce chemicals with antimicrobial properties (Tan and Zou 2001).

The ability of kojic acid to suppress tyrosinase, the enzyme responsible for hyperpigmentation, has led to its inclusion in various cosmetic formulations, such as creams, lotions, and soaps, to mitigate the wrinkle effects of sun exposure. Saeedi et al. (2019) noted that it is also used to avoid the browning of food. This metabolite and its derivatives are in high demand due to their potential utility and widespread use in the cosmetics, personal care, food, agricultural, pharmaceutical, medical, and chemical industries. *Aspergillus oryzae* and *Aspergillus flavus* frequently produce kojic acid (Ola et al. 2019).

The authors of this study intended to evaluate and introduce some beneficial morphological and palynological characteristics of *C. erectus* in Egypt. To demonstrate the histological presence of this species' endophytes, which may produce active chemical compounds with potential therapeutic applications. Also, to illustrate the anatomical structure of the stems and leaves of *C. erectus*.

2 Material and methods

2.1 Plant material

Data for this study of the Egyptian species *C. erectus* L. were based on collected specimens from the campus of South Valley University (SVU), Qena Governorate, Egypt. Collections were gathered from two sites with the coordinates [Latitude 26.19208o and Longitude 32.74527o]. Voucher specimens and permanent slides were deposited in the South Valley University-Qena Herbarium (QNA, a proposed acronym). Voucher specimens and slides were investigated and photographed by the author. According to Stace (2007) and the website https://wfoplantlist.org, nomenclature and synonyms were reviewed for taxonomic attributes.

2.2 Methods

Plant parts were evaluated by neck eyes. Measurements were taken with a ruler directly or, for finer details, by an ocular piece under a dissecting microscope.

2.3 Light microscopy investigations (LM)

An Olympus-light dissecting microscope was used to study vegetative leaves and the stem. This microscope has an

ocular-equipped × 20 eyepiece. The ocular piece was calibrated by a standard graduated slide [graduation equals 1 mm (about 0.04 in)]. Digital photographs were captured using the Samsung ST72 HD digital camera.

Good leaf portions were inserted in test tubes and treated with lactic acid 88% in a water bath at 100 °C to remove the cuticle and soften the leaf tissue to investigate foliar micromorphology (Clarke 1960). This made it simpler to prepare slides with Canada balsam-mounted epidermal layers from the leaf's abaxial and adaxial sides. A study was done on stomata features and trichome types (Table 1).

Only young, robust leaves and stems were chosen for the anatomical studies. Plant parts were collected from the fifth node upwards on the vegetative stems and leaves. They were preserved in 70% alcohol and dehydrated in a series of ethyl alcohols; the fresh specimens were immersed in a formalin-acetic acid alcohol (FAA) solution for at least 48 h (about two days). The sections were cut using a rotary microtome, dyed with safranin fast green, and mounted in Canada balsam (Johansen 1940). A Labomed-Labo America, Inc. LM was used to analyze sections of permanent slides at magnifications of 4, 10, and 40 to provide the best possible clarity. ToupView digital camera attached to Leica DM1000 microscope was used for microphotography. Table 2 lists the values found for the various anatomical characteristics.

Samples from the mature anthers of the flowers were collected for palynology research. The sample was placed on a clean slide, briefly brought to a boil in water, rehydrated in a 10% KOH aqueous solution, mounted in glycerin jelly, and sealed with paraffin wax. Using a light microscope (Labomed-Labo America, Inc.) with a magnification of 100, permanent slides were inspected. Micrographs were taken using a Leica DM1000 microscope with a ToupTek ToupView digital camera. Using ocular tools, pollen grain measurements were based on an average of 15–20 readings for each P- and E-diameter for each sample of 10–15 pollen grains (Table 1).

2.4 Scanning electron microscopy investigations (SEM)

Healthy leaf portions were selected for trichome and stomata examination, mounted onto clean, marked holders using double-sided self-adhesive tape, scanned, and photographed by JOEL JSM-5500 LV, accelerated by a voltage of 15 kV at the SEM Unit, South Valley University-Qena, Egypt.

Pollen grains from unacetolyzed anthers mounted on metallic stub holders were used for palynology research. The anthers specimens were attached to the holders with double-sided self-adhesive tape. Each sample was coated with gold using a JEOL JFC 1100 E ion sputtering equipment before being analyzed using a JEOL JSM 5400 LV scanning electron microscope at Assiut University in Egypt with an acceleration voltage of 15 kV.

2.5 Terminology

The terminology of vegetative description was according to Stearn (1983). The pollen shapes, size, and surface sculpture terminology were followed by Punt et al. (2007). The author referred to the colpus length as "terminal" when the colpus length was 0.8–0.9 times the total polar axis length and "subterminal" when it was 0.7–0.8 times of the polar axis (Kamel et al. 2019).

2.6 Isolation of endophytic fungi

Endophytic fungi were isolated from plant leaves using the method described by Rossman et al. (1998). The leaves of *C. erectus* were gently cleaned under running water to remove dust. After washing, leaves were divided into segments (1 cm (about 0.39 in) long and diameter with midrib). The surfaces of the segments were sterilized by immersion in 75% ethanol for one minute, 5% available chlorine sodium hypochlorite for two minutes, and another sterilization with 75% ethanol for 1 min. After three washes with sterile distilled water, the segments were dried between sterile filter sheets. Four segments were inoculated on a potato dextrose agar (PDA) plate that had received chloramphenicol treatment. The plates were incubated at 28 °C for 1–2 weeks, and the growing fungi were identified as described by Moubasher (1993).

2.7 Plant and fungal extracts preparation

The first step in making the plant extract involved washing and cleaning *C. erectus* leaves with distilled water. The leaves were then air-dried for four days before milling into a fine powder. Ten g of the prepared leaf powder was added to 100 mL of dist. H2O, ethanol, and methanol while shaking for 24 h. The extract solutions were filtered through Whatman No.1 filter paper for purification. The ethanol and methanol extracts could dry at room temperature until constant weight. Dimethylsulfoxide (DMSO) was used to dissolve the resultant dried residue, which was then refrigerated.

The fungal isolate (*A. flavus*) was cultivated on PDA medium at 28 °C for seven days to prepare a crude extract from endophytic fungi. Afterward, a 250 ml (about 8.45 oz) Erlenmeyer flask containing 50 ml (about 1.69 oz) of PDB was cultured with an 8 mm (about 0.31 in) disc of the growing culture of the fungal species and incubated for 15 days (about two weeks) at 28 °C on a rotational shaker at 160 rpm. The culture broth was filtered using Whatman filter paper after the incubation period, and the filtrate was extracted using chloroform

Table 1 Macro- and micro-morphological characters of *Conocarpus erectus*

Plant part	*Characters*
Habit	Shrubs to trees
Stem outline	Convex triangular
Hairiness	Glabrous to few hairy
Leaves	
1. *LMN shape*	Lanceolate
2. *LMN L. cm*	6.2–9.1
3. *LMN W. cm*	1.4–2.2
4. *LMN L./W. ratio*	3.6–5.3 times
5. *Margin*	Entire to integerrimus
6. *Apex*	Acute
7. *Base*	Attenuate
8. *Petiole L. mm*	2–5
9. *Bract shape*	Lanceolate
10. *Bract hairiness*	Hairy
11. *Bract L. mm*	1–4
Trichomes types	
1. *Type*	1. Simple/ 2. Glandular
2. *Basal origin cell*	1. Unicellular base cell/ 2. Short stalk cell
3. *Gland structure*	Gland unicellular to multicellular
Stomata structure	
1. *STCX L.* µm	26.6–37.5
2. *STCX W.* µm	17.3–25.0
3. *STP shape*	Narrowly elliptic to ovate
4. *STP length*	Short
5. *Rims*	Absent
Pollen grains	
1. *Size*	Small
2. *Shape*	Perprolate to prolate
3. *Polarity*	Isopolar
4. *Symmetry*	Symmetric
5. *P- axis* µm	12.9- 18.66 (15.85)
6. *E- axis* µm	9.0- 12.58 (10.73)
7. *P/E ratio*	1.20- 2 (1.52)
8. *Aperture type*	6-heterocolpate
9. *Colpi shape*	Linear and rhomboidal
10. *Colpi L.* µm	10.86- 14.82 (12.79)
11. *Colpi W.* µm	0.34- 2.58 (0.97)
12. *ENDAP shape*	Lolongate
13. *ENDAP size* µm	2.97–3.67 × 1.25–2.0 µm
14. *Apocolpium diameter* µm	4.13–7.5
15. *CPMB sculpture*	Granulated
16. *CPMG sculpture*	Psilate to rugulate
17. *Tectum*	Psilate to rugulate, scarce perforations mesocolpium

*Abbreviations: *LMN.* Lamina, *STCX.* Stomata Complex, *STP.* Stomata Pore, *ENDAP.* Endoaperture, *CPMB.* Colpus Membrane, *CPMG.* Colpus Margin

(1:1, v/v) while being constantly shaken for 24 h. At room temperature, the organic phase evaporated. Until it reached a consistent weight, the concentrated extract was kept in complete darkness (Silva et al. 2011). The obtained crude extract was DMSO-dissolved and refrigerated.

Table 2 Anatomical structural characters of stem and leaves of *C. erectus*

1. STEM	*Characters*	2. LEAF	*Characters*
Outline	Triangular	Midrib region thickness µm	750–800
Size (L. x W. mm)	2.25–2.30 × 1.72–1.75	Margin region thickness µm	
		1. *PLS (Ad.)*	80–125
		2. *PLS (Ab.)*	30–37.5
		3. *Spongy layer*	130–232.5
Cuticle thickness	Normal	Cuticle thickness	Normal (c. 5.0 µm)
Epidermis		Epidermis	
1. *Shape*	Elongated	1. *Shape*	Cubic-shaped & elongated
2. *Orientation*	Radially (parallel)	2. *Orientation*	Perpendicular & parallel
3. *EPC* L. µm	15.0–22.5	3. *EPC* L. µm	12.5–20
4. *EPC* W. µm	7.5–12.5	4. *EPC* W. µm	10–20
Cortex structure			
1. *Cells type*	Parenchyma		
2. *Rows no*	8–11		
3. *Thickness* µm	112.5–200.0		
4. *Lower Corner-side thickness* µm	390.0- 462.5		
Vascular structure		Vascular structure	
		I. Marginal VSC-ST	
1. *VSC-ST*	Complete cylinder	1. *Shape*	Masses
2. *XRW no*	1 & 2–4	2. *Diameter* µm	32.5–57.5
3. *XVS no*	1–3 & 4–9	II.Mesophyll VSC-ST	
4. *XYL thickness* µm	62.5–1.62.5	1. *Shape*	Semi-cylinder (arc)
5. *OTPH presence/absence*	+	2. *XRW no*	11–15
6. *OTPH shape*	Strip-shaped	3. *XVS no*	1–4
7. *OTPH thickness*	30.0–62.5	4. *XYL size* (L. x W.) µm	400–430 × 60–80
8. *INPH presence/absence*	+	5. *OTPH presence/absence*	-
9. *INPH shape*	Masses/patches	6. *INPH presence/absence*	+
10. *INPH diameter*	25.0–30.0	7. *INPH thickness*	27.5–42.5
Pith structure			
1. *Types of cells*	Parenchyma		
2. *Size* (L. x W. mm)	1.27–1.37 × 0.82–0.87		

*Abbreviations: *EPC L.* Epidermal Cells Length, *EPC W.* Epidermal Cells Wide, *VSC-ST* Vascular Structure, *XRW no.* Xylem Rows number, *XVS no.* Xylem Vessels number, *XYL* Xylem region, *OTPH* Outer Phloem, *INPH* Inner Phloem, *PLS* Palisade tissue, *Ad.* Adaxial & Ab. Abaxial

2.8 Preparation of spore suspension

The three fungal strains, *Geotrichum candidum* (Accession number: OL960606), *Neoscytalidium dimidiatum* (OL960610), and *Scopulariopsis coprophila* (OL960621) tested in this study were isolated in our laboratory (Applied and Environmental Microbiology, South Valley University). The fungal isolates were cultured on PDA medium at 28 ºC for seven days.

Spores were collected from fresh cultures, added to 10 mL of saline water (0.90% w/v of NaCl), and vortexed for 5 min. The concentration of spores in the suspensions was counted using a hemocytometer chamber (2×10^6 spores/mL).

2.9 Microtiter plate assay

The antifungal efficacy of extracts was evaluated using a sterilized 96-well plate: microdilution method (Ivanova et al. 2013). The antifungal capability of plant extracts and an endophytic fungus (*A. flavus*) was evaluated using the first five rows of a microtiter plate, and the last two were used as positive and negative controls. The extract was then added in 50 µL portions to the first well in the plate row after each well received 50 µL of sterile Potato Dextrose Broth (PDB). Each of the first five rows of wells underwent a sequential dilution process. Each well was filled with a 5 µL resazurin solution and a 5 µL fungal suspension. An indication of fungus growth was resazurin. The wells appeared with a

blue-colored solution, indicating the tested extract inhibition and antifungal effect. In contrast, a pale pink to a colorless solution resulted from microbial growth or the lack of inhibition. Fifty µL of PDB, five µLof resazurin, and five µLof fungal suspension were used as the positive control (used to verify the viability of the fungus culture), whereas 50 µLof PDB and five µLof resazurin were used as the negative control (used to check the sterility of the working environment and solutions). The microtiter plates were then incubated for five days at 25 ± 2 °C. The lowest concentration of extract that inhibits the development of microorganisms is known as the minimum inhibitory concentration (MIC).

2.10 Analysis of bioactive components

According to antifungal results, aqueous and crude extracts of *C. erectus* leaves (ethanol and methanol) and a crude extract of *A. flavus* were subjected to analysis for the presence of active components by high-performance liquid chromatography (HPLC) and Gas chromatography-mass spectrometry (GC–MS), respectively. The procedures of HPLC analysis were carried out according to the method of Kim et al. (2006) at the Central Lab. of Food Industries and Nutrition Institute, National Research Centre, Giza 12622, Egypt. A quick-fit conical flask held the sample, and 20 ml of 2 M NaOH was placed. After flushing the flasks with N2, stoppers were added. The pH was changed to 2 by adding 6 M HCL after the flasks had been shaken for 4 h at room temperature. The supernatant was obtained after centrifuging the contents of each flask at 5000 rpm for 10 min. Two extractions of phenolic compounds were carried out using 50 ml each of ethyl ether and ethyl acetate (1:1). After separating the organic phase and evaporating the solvent at 45 °C, the residues were re-dissolved in 2 ml of methanol and subjected to HPLC analysis.

An Agilent Technologies 1100 series liquid chromatograph outfitted with an autosampler and a diode array detector was used to conduct the HPLC analysis. The analytical column was a Phenomenex, Torrance, California, Eclipse XDB-C18 (150 × 4.6 µm; 5 µm) with a C18 guard column. The mobile phase comprised the Acetonitrile (solvent A) and 2% acetic acid in water (solvent B). The gradient program was as follows: 100% B to 85% B in 30 min, 85% B to 50% B in 20 min, 50% B to 0% B in 5 min, and 0% B to 100% B in 5 min. The flow rate was maintained at 0.8 ml/min for the entire run time of 60 min. The injection volume was 50 µl, and flavonoids, benzoic acid derivatives, and cinnamic acid derivative peaks were concurrently seen at 360 nm and 280 nm, respectively. Before injection, all materials were filtered with an Acrodisc 0.45 µm syringe filter from Gelman Laboratory in Michigan. Peaks were located by matching UV spectra and retention times, then contrasted with the standards. The concentrations were calculated by proportional analysis (external standardization technique), comparing the peak area (PA) of the analyte in the unknown to the peak area of a known amount (C) of the standard:

$$C_{standard} = C_{unknown}$$

$$PA_{standard} = PA_{unknown}$$

The crude extract of *A. flavus* was screened in the Department of Chemistry, Annex (B), Faculty of Science, Assiut University, Assiut 71,516, Egypt. The Thermo Scientific TRACE GC UltraTM gas chromatograph was used to conduct endophytic fungal extract analyses. An MS Polaris QQuadrupole Ion Trap (Thermo Electron) was coupled to a J & W Scientific Fisons, Folsom, CA, bonded silica column VB5 (5% phenyl, 95% methylpolyxiloxane, 30 m at 0.25 mm internal diameter, 0.25 µm film thickness). The injector was run at 250 °C, while the interface was run at 300 °C. The following settings were entered into the oven's controller: 50 °C to 250 °C in (4 °C/min). A 1 ml/min flow of helium served as the carrier gas. In split mode (1:20), the sample volume (1 µl) was injected. The mass spectrometer settings were EI = 70 eV, and mass range = 10–350 amu. Their identities were confirmed by comparing the retention periods and mass spectra of the extracts of endophytic fungus components to those of verified samples (analytical standards from a data database) (Bayoub et al. 2010) comparing the retention periods and mass spectra of the extracts of endophytic fungus components to those of verified samples (analytical standards from a data database) (Bayoub et al. 2010), their identities were confirmed.

3 Results

3.1 Structural observations

Conocarpus erectus was glabrous to a few hairy evergreen shrub to tree; the stem was brown with a convex and triangular form. The indumentum on the leaves were few, the leaves were appressed pubescent earlier, then glabrescent, and the trichomes were less on the adaxial surface; leaves were light green, alternate; lamina lanceolate (Fig. 1, a), with two prominent nectarous glands basally (Fig. 1, d & e); glands bowl-shaped, papillate (Fig. 2, a & b); lamina size 6.2–9.1 × 1.4–2.2 cm [L = 3.6–5.3 times W] (Fig. 1, b); margin entire to integerrimus; apex acute; base attenuate, petiolate or subsessile; petiole 2–5 mm long; ebracteate to bracteate; cauline leaves commonly with minute bracts (Fig. 1, c); bracts were lanceolate, short, hairy on both surfaces and 1–4 mm long Table 1.

Simple and glandular hairs covered the leaves. Simple trichomes were sparse, slender-shaped, appressed, and

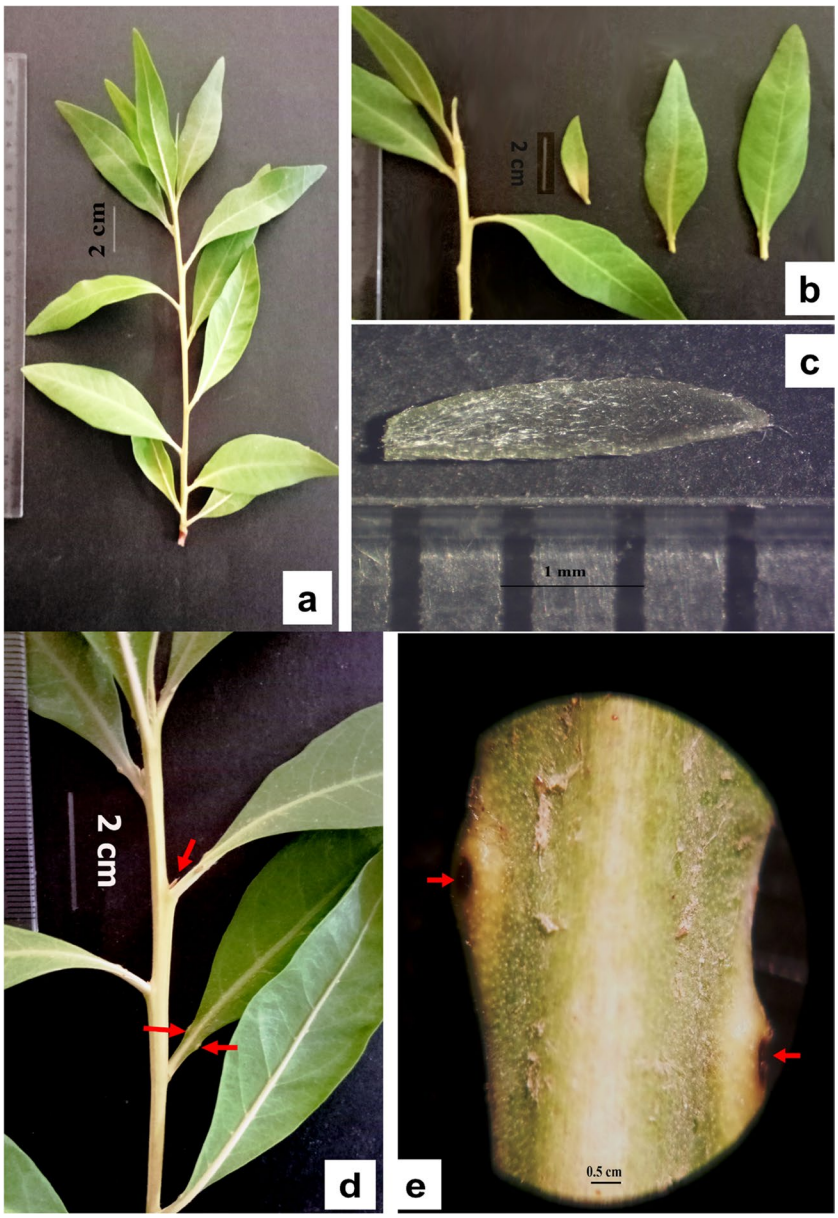

Fig. 1 Leaves of *Conocarpus erectus* (**a**) lamina shape and arrangement on stem (**b**) leaves of different sizes (**c**) bract shape and hairiness (**d**) bract and the leaf base showing the two nectarous glands (**e**) magnification at 20 showing the position and shape of the basal glands of leaves [a, b, and d: bar = 2 cm; c: bar = 1 mm; e: bar = 0.5 mm]

progressed from a swelling unicellular base (Figs. 2c, and 3, e). Glandular hairs (Fig. 2, d) are seen on the adaxial surface of leaves; their heads were circular or capitate-shaped, unicellular, or multicellular, and submerged within short stalks on the epidermal cells (Fig. 3, c & d). The leaves were amphistomatal, with hyphae of endophytic fungi visible on both leaf surfaces (Fig. 3); the stomata pore was short, narrowly elliptic to ovate, with no rims surrounding the pore (Fig. 2 c and d); and the stomata complex size was 26.6–37.5 × 17.3–25.0 µm Table 1.

The leaf transverse section, as shown in Fig. 3a, was composed of a layer of epidermal cells; it is 12.5–20.0 × 10.0–20.0 µm, covered with a normal layer of the cuticle (c. 5.0 µm thick), the cells of the epidermis are cubic-shaped or elongated and have been oriented perpendicular to or parallel to the section direction (Fig. 3, c, d, and e). The margins are made up of palisade and spongy tissues; the palisade layer on the adaxial surface was two rows thick, 80–125 µm thick, and thinner on the abaxial surface (one row of palisade cells, 30.0–37.5 µm thick); the spongy tissue included druses; its thickness was 130.0–232.5 µm, and it intermixed with vascular masses, which consisted of a few xylem vessels and some phloem and had a diameter of 32.5–57.5 µm. The main vascular tissue was a semi-cylinder or an arc of xylem rows and inner phloem (Fig. 3, b); the xylem rows number ranged from 11–15; each xylem row was of 1–4 vessels, and the xylem region size was 400–430 × 60–80 µm; the innermost phloem thickness was 27.5–42.5 µm. The midrib's total thickness was 750–800 µm, with dispersed druses, particularly on the

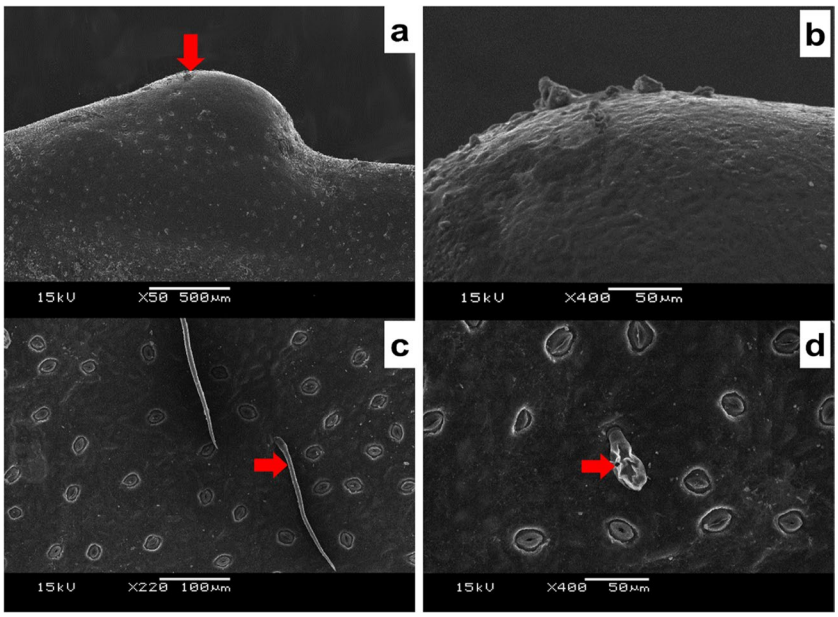

Fig. 2 SEM-micrographs in *Conocarpus erectus* leaves showing (**a**) the nectarous bowl-shaped gland at the leaf base "arrowed"; (**b**) magnification of the nectar gland surface reveals papillae and rugulations; (**c**) the stomata complex structure and the unicellular-based raised unicellular, appressed trichomes; and (**d**) an arrow reveals the glandular hair

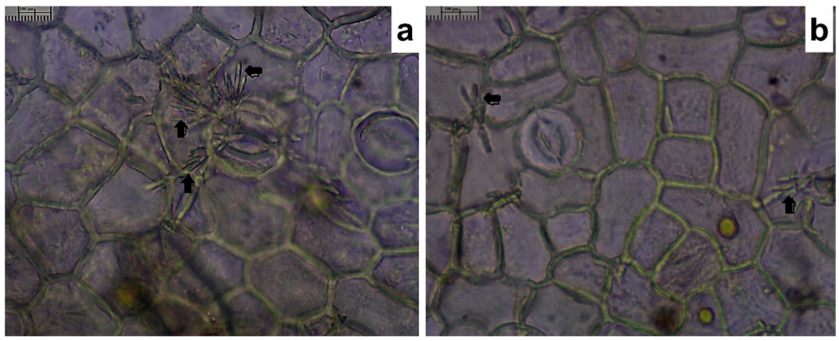

Fig. 3 LM-micrographs of the adaxial and abaxial surfaces of leaves of *Conocarpus erectus*; arrows revealed the structure of endophytic fungi (*Aspergillus flavus*): (**a**) on the adaxial surface, fungal hyphae surrounded the stomata complex; and (**b**) on the abaxial surface, fungal hyphae penetrated the epidermal cells and surround stomata [mag. x = 40; one bar of standard slide = 100 µm]

abaxial surface (Fig. 5, c). Table 3 indicated the presence of phenolic compounds and idioblasts in *C. erectus* leaf tissues; Fig. 5c showed the phenolic-colored epidermal cells on leaf surfaces, and Fig. 5d showed a blue color accumulated in the palisade tissue.

The stem transverse section outline was triangular, 2.25–2.30 × 1.72–1.75 mm size; the epidermis was a single layer of radially elongated cells, 15.0–22.5 × 7.5–12.5 µm size, covered by a normal-thickened cuticle layer and simple trichomes are arisen (Figs. 4 and 5, a); the cortex was of 8–11 horizontal rows of parenchyma cells, with scattered druses, 112.5–200.0 µm thick at the circumference of the section; endophytic fungi mycelia are observed running through the parenchyma of the cortex (Fig. 6, c); cortical tissue at two lower corners of the sector was more thickened and with more druses (Fig. 5, b), corner-cortex was 390.0–462.5 µm thick (Fig. 4, a); vascular tissues were continuous as a complete cylinder; Secondary xylem elements consist of xylem vessel rows, these arranged singly or in nearby 2–4 aggregates; vessels number in a single xylem row was 1–3, more (4–9 vessels) in the aggregated ones (Fig. 4, b); xylem region thickness was 62.5–1.62.5 µm in Table 2, vessels were intermixed with fibres at the secondary growth part and with parenchyma at the innermost primary growth part; the phloem was in two regions, the outermost and the innermost; druses are also

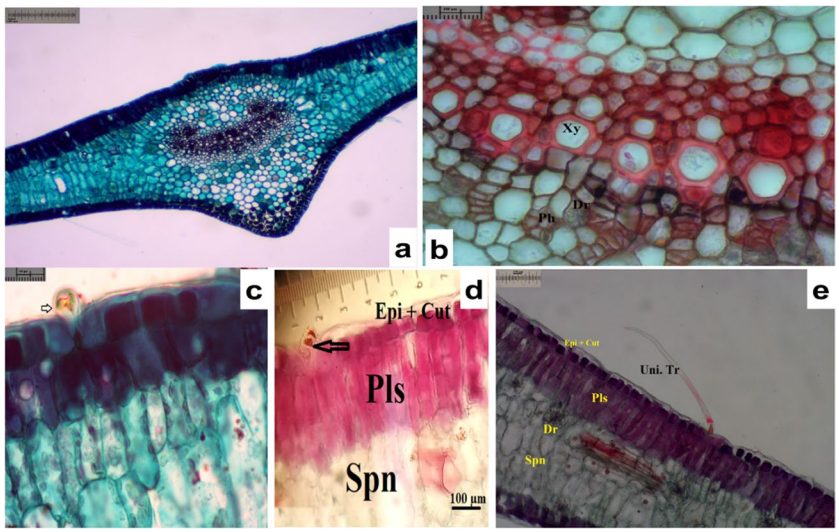

Fig. 4 LM-micrographs showing the leaf anatomical structure of *Conocarpus erectus* (**a**) general shape of leaf T.S. sector [mag. x = 4; one bar of standard slide = 100 µm] (**b**) the internal structure revealed the vascular arc of phleom (Ph) with druses (Dr) and xylem rows (Xy) [mag. x = 10; one bar of standard slide = 100 µm]; (**c**) arrows revealed the unicellular gland of the glandular trichome at the adaxial surface [mag. x = 40; one bar of standard slide = 100 µm] (**d**) The adaxial surface revealed epidermal cells covered by the cuticle (Epi + Cut), palisade cells (Pls), and spongy cells (Spn), and an arrow showed the multicellular gland of the glandular trichome [mag. x = 10; one bar of a standard slide = 100 µm]. (E) The margin region of the leaf showed the unicelluar simple trichomes on the adaxial surface and the internal tissues [mag. x = 10; one bar of a standard slide = 100 µm]

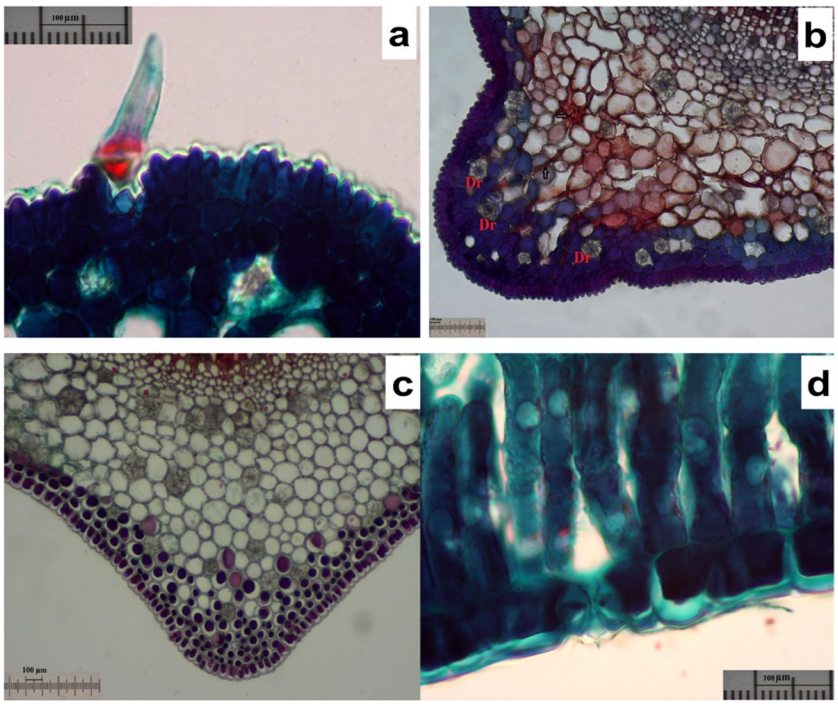

Fig. 5 LM-micrographs showing the phytochemical components in the stem (**a** and **b**) and in the leaf (**c** and **d**) sectors of *Conocarpus erectus* appearance (**a**) deep blue colour accumulation in the epidermal cells and hypodermis; **b** violet colour accumulation and many idioblasts (Druses; Dr.) deposited at the lower corner-side of the section. **c** High violet colour accumulation and many idioblasts (Druses; Dr.) deposited at the abaxial epidermis and hypodermis at the midrib region of the leaf. **d** Deep blue colour accumulation within the palisade cells at the abaxial surface and stoma structure is revealed [a & d: mag. x = 40, b & c: mag. x = 10; one bar of a standard slide = 100 µm]

formed in the phloem. The outer phloem was strip-shaped, with a thickness of 30.0–62.5 µm, while masses/patches of the inner phloem were smaller in diameter, 25.0–30.0 µm diam.; the pith was centered, started by the ending border outline of the vascular tissues; it consisted of normal storage parenchyma cells, 1.27–1.37 × 0.82–0.87 mm size, with druses distributed through it. Figure 5 shows the colored phenolic compounds that accumulated in the epidermis

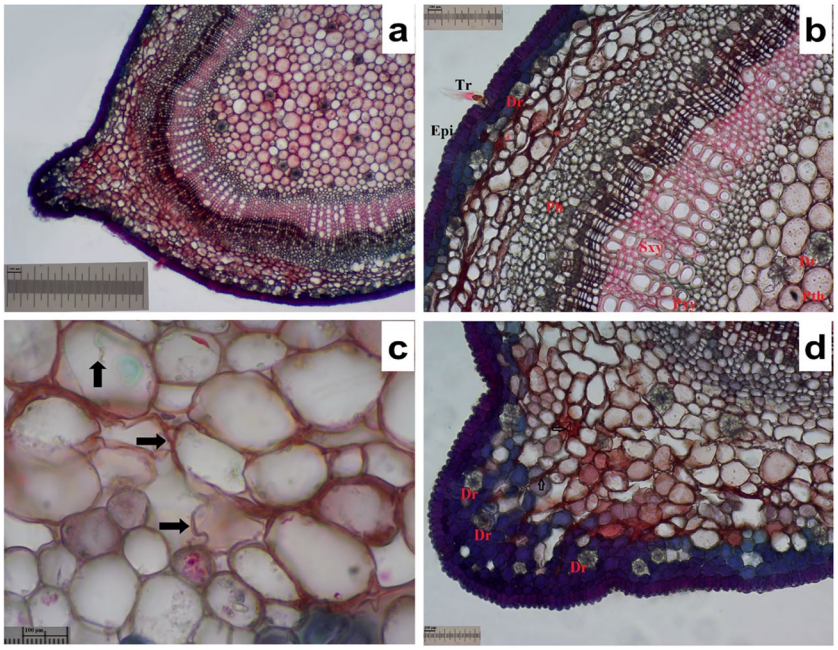

Fig. 6 LM-micrographs showing the stem anatomical structure of *C. erectus* (**a**) general outline of stem sector [mag. x = 4; one bar of standard slide = 100 µm] (**b**) the internal structure reveals the epidemis with trichomes, cortex with druses (Dr), phloem (Ph), secondary xylem (Sxy), and primary xylem (Pxy), and pith (Pth) with druses [mag. x = 10; one bar of standard slide = 100 µm]; (**c**) arrows reveal the running mycelium of endofungus (*Aspergillus flavus*) within the parenchyma cells of the cortex [mag. x = 40; one bar of standard slide = 100 µm] (d) The lower corner-side of the sector reveals a larger thickness of the cortex region with many druses [mag. x = 10; one bar of a standard slide = 100 µm]

Table 3 Phytochemical components' histological appearance of stem and leaves of *C. erectus*

Phytochemical histological appearance of:	
1. *Idioblasts type*	Crystals (Druses)
2. *Idioblasts' occurrence in tissues of:*	2.a. Stem [hypodermis (cortex) + phloem + pith] 2.b. Leaf [hypodermis + sponge cells of margin + parenchyma of midrib]
3. *Phenolic compounds accumulation in tissues of:*	3.a. Stem [epidermal cells + hypodermis + cells of cortex lower corner-side] 3.b. Leaf [epidermal cells (Ad. & Ab.) + palisade cells (Ad. & Ab.) + lower mesophyll parenchyma cells] 3.c. purple, violet or blue color accumulation in cells

and hypodermis cells of the *C. erectus* stem. Table 3 summarises the appearance of these compounds and other idioblasts (druses).

Pollens were monads; dimensions of the polar and equatorial axes and aperture size were measured and illustrated in minimum–maximum (average) values. Pollen small: P = 12.9–18.66 (15.85) µm, E = 9.0–12.58 (10.73) µm; isopolar, radially symmetric; outline: triangular-circular-6-lobate in polar view, broadly elliptic in equatorial view with flattened and slightly emarginate ends (Fig. 7, a & b); subprolate to prolate, P/E = 1.20–2 (1.52). Table 1 showed that the grains were 6-heterocolpate (Fig. 7, c), in which three simple colpi alternated with three compound ones, elongate endoaperture were slightly observed (Fig. 7, d), endoaperture size was 2.97–3.67 × 1.25–2.0 µm [L x W]. Colpi were linear and rhomboidal (in wider colpi) with acute to rounded ends, 10.86–14.82 (12.79) µm length, and varied in width, 0.34–2.58 (0.97) µm; three terminal colpi represented 0.8–0.96 times of the polar axis alternated with shorter, subterminal three ones, represented 0.8 (0.77–0.79 times of the P-axis); a bridge was observed from sexinous protrusions (Fig. 7, d); apocolpium narrow (Fig. 7, e), 4.13–7.5 µm in diameter; Fig. 7e & f illustrated the granulated colpi membrane, margin psilate to rugulate; tectum psilate to rugulate; scarce perforations in the mesocolpium were observed (Table 1).

3.2 Collection of endophytic fungi

Aspergillus flavus was isolated from healthy leaves of *C. erectus.*

3.3 Microtiter plate test

A microtiter plate assay was performed to detect the activity of three extracts of *C. erectus* and an extract of an endophytic fungus (*A. flavus*) in terms of MIC. The MIC of the extract is the minimum concentration required for the inhibition of fungal growth. The values of MIC for different

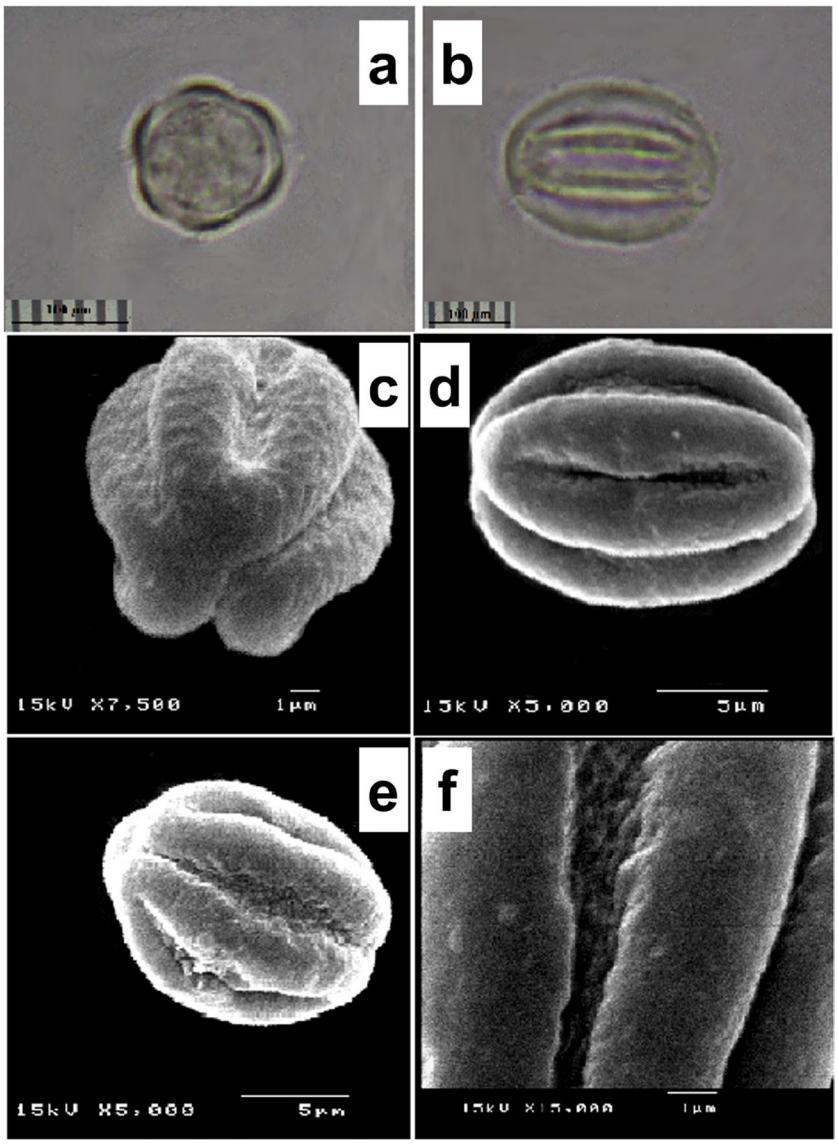

Fig. 7 Pollen grains of *Conocarpus erectus* (**a**) LM-micrograph showing the polar view; (**b**) LM-micrograph showing the equatorial view [in a and b: magnification x = 100; bar = 100 µm] (**c**) SEM-micrograph showing the polar view; tectum clears that psilate at the apocolpium and regulates it in the mesocolpium; triangular-circular-6-lobate outline; (**d**) SEM-micrograph showing the equatorial view and the terminal, subterminal colpi, and the bridge at the colpi margin. **e** SEM-micrograph showing an oblique equatorial view showing the granulated colpus membrane, sparse perforation in the mesocolpium region, and narrow apocolpium region, and (**f**) magnification at × 15.000 showing the rugulate colpus margin and psilate tectum

extracts of *C. erectus* and *A. flavus* against opportunistic fungi, *Geotrichum candidum*, *Neoscytalidium dimidiatum*, and *Scopulariopsis coprophila* are shown in Fig. 8.

Figure 8a showed the bioassay results against *Geotrichum candidum*. The results revealed that extracts 2, 3, and *A. flavus* inhibited the growth of the yeast at a MIC of 1.25×10^3 µg/mL. On the other hand, fluconazole exhibited antifungal activity and inhibited mycelial growth at a MIC of 0.31×10^3 µg/mL. It was noted that the resazurin dye indicator was reduced in two stages, from resazurin to resorufin to hydroresorufin, which appeared colorless.

Figure 8b: Extracts 2 and 3 displayed the same antifungal ability against *Neoscytalidium dimidiatum*, which exhibited a MIC1.25×103 µg/mL. Extracts of *A. flavus* and fluconazole showed identical antifungal activity and inhibited mycelial growth at a MIC of 0.63×10^3 µg/mL.

Figure 8b: *Scopulariopsi scoprophila* was sensitive to Extract 2, which exhibited antifungal activity at a MIC of 1.25×10^3 µg/mL. Extract 3 and *A. flavus* showed the same antifungal activity and displayed MIC of 2.5×10^3 µg/mL. Fluconazole inhibited the growth of this fungus at a MIC of 0.31×10^3 µg/mL.

From the above results, powdered Extract 2 extracted by 70% ethanol and *A. flavus* extracted by chloroform were the best natural products to potentiate the antifungal activity against the tested fungi.

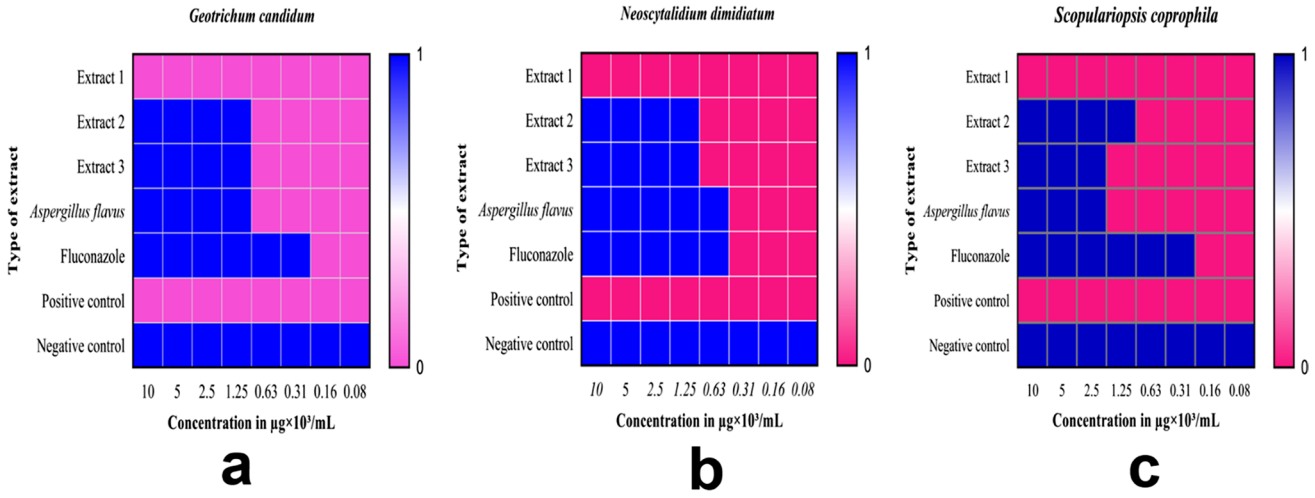

Fig. 8 MIC of four extracts against pathogenic isolates of *Geotrichum candidum*, *Neoscytalidium dimidiatum,* and *Scopulariopsi scoprophila* Extract 1: aqueous *Conocarpus erectus* leaves, Extract 2: extract with 70% ethanol, Extract 3: extract with 95% methanol. 1: inhibition, 0: non-inhibition

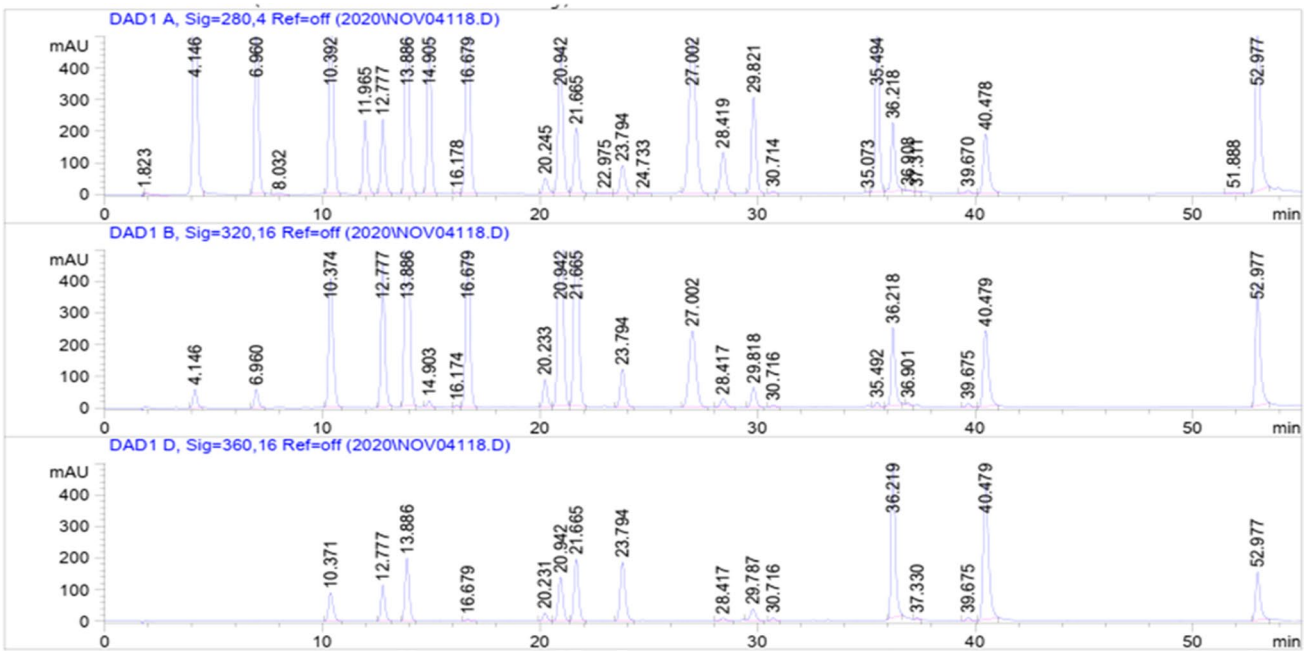

Fig. 9 HPLC standard curves of chemical-standard compounds surveyed in *Conocarpus erectus* leaves

3.4 Determination of bioactive secondary metabolites

A crude extract of *C. erectus* leaves was screened by HPLC to determine the bioactive materials with antimicrobial properties (Fig. 9). Sixteen compounds were detected in the crude extract at different concentrations. Gallic acid, rutin, and rosmarinic acid were the major components represented by 3230.30, 1013.68, and 120.55 µg/g Table 4.

Kaempferol, sinapic, and apigenin were identified in the extract of *C. erectus* leaves with 68.51, 20.55, and 24.51 µg/g.

Table 4 Bioactive compounds detected in HPLC analysis of *C. erectus* leaves

Compound	Concentration (µg/g)
Gallic acid	3230.30
Protocatechuic	17.00
p-hydroxybenzoic	8.06
Catechin	9.95
Syringic	16.58
Vanillic	4.38
Ferulic	5.54
Sinapic	20.55
Rutin	1013.68
Rosmarinic	120.55
Cinnamic	1.89
Qurecetin	16.02
Apigenin	24.51
Kaempferol	68.51
Chrysin	2.66

Protocatechuic, syringic, quercetin, and catechin were found in the extract of *C. erectus* leaves at 17.00, 16.58, 16.02, 9.95 µg/g, respectively.

p-hydroxybenzoic, Ferulic, Vanillic, Chrysin, and Cinnamic with 8.06, 5.54, 4.38, 2.66, and 1.89 µg/g, respectively, were recorded in the crude extract of *C. erectus* leaves.

Endophytic fungi *A. flavus* was isolated from the medicinal plant *C. erectus*. The endophytic fungus was cultured on 100 ml PDB media in 1 L Erlenmeyer flasks for three weeks. The culture of the fungus was extracted with chloroform. GC–MS analyzed the chloroform crude extract to determine the chemical metabolite content. Based on the results obtained from the analysis, *A. flavus* was noted to produce 44 bioactive components (Fig. 10). It produced a significant compound, kojic acid, with the highest content of 98.551%, which is known to exhibit antimicrobial activity. From the obtained results, 15 compounds were observed to possess antimicrobial activity: 1,2-Benzenedicarboxylicacid,bis(2-ethylhexyl)ester, 2-(2-Aminopropyl)phenol, 4-(2-Amino-1-hydroxypropyl) phenol, 9-Hexacosene, Actinobolin, Bis(2-ethylhexyl) phthalate, Cis-Aconitic anhydride, Decane, Dl-Mevalonic acid lactone, Dl-Phenylephrine, Dotriacontane, E-14-Hexadecenal, n-Octadecane, Tetracosane, and Trans-Limonene Oxide, with values fluctuating between 0.001–0.294% (Table 5).

4 Discussion

The evergreen shrub or tree known as the buttonwood (*Conocarpus erectus* L.) can be found in Egypt. Stace (2007) also describes it as like or found in mangroves. Two bowl-shaped nectarous glands are located at the leaf's base. These two glands were first observed on the petiole of *C. erectus* by Elias (1983) and Koptur (1992). A pair of elongated, swollen, hollow nectaries was discovered by Diaz-Castelazo et al. (2005) on both sides of the leaf petiole of *C. erectus*. In *C. lancifolius*, however, they were discovered by Redha et al. (2011) due to a pair of nectaries located outside of the flowers on the petiole.

In this study, there were two distinct kinds of indumentum leaves. These trichomes were both glandular and

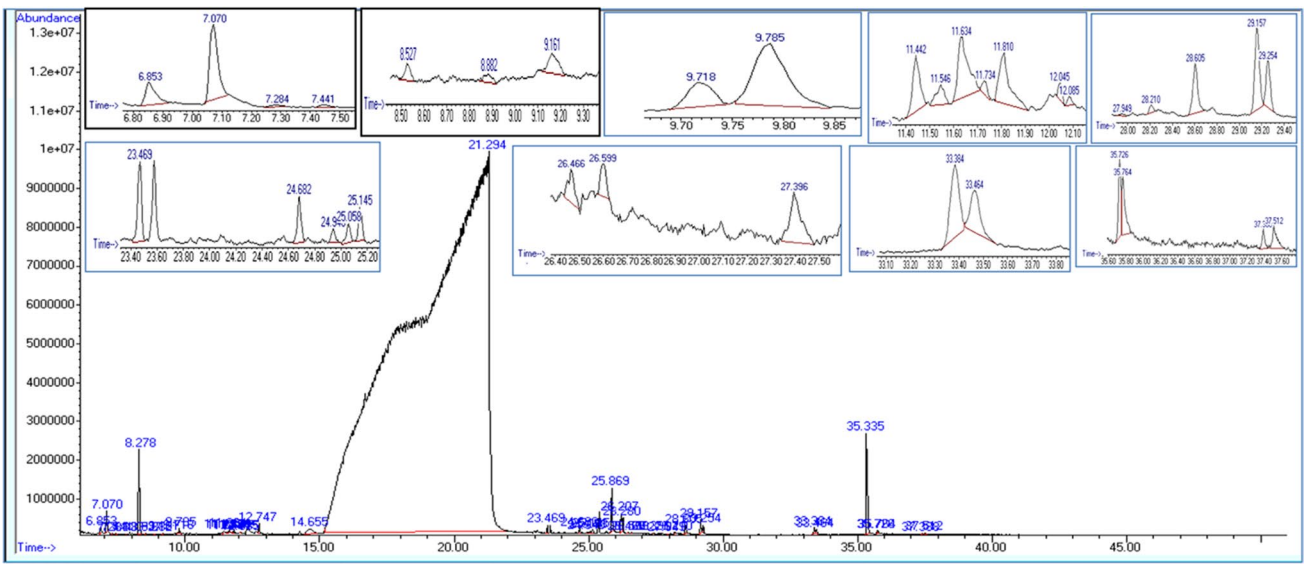

Fig. 10 Screening chromatograms of *Aspergillus flavus* extract

Table 5 Secondary metabolites detected in GC–MS analysis of *Aspergillus flavus*

Analyte/Parameter	Value (%)
Dimethylformamide	0.002
(R)-(-)-2-Amino-1-propanol	0.002
1,2,4,5-Tetra-O-methyl-D-mannitol	0.005
1,2-Benzenedicarboxylicacid,bis(2-ethylhexyl) ester	0.013
2-Hydroxy-butanedial	0.011
2-(2-Aminopropyl)phenol	0.002
2-[(1-phenyl-1-hydroxy)methyl]-3,5-dimethylcyc lohexanoneisomer	0.001
2-Formylhistamine	0.002
2-Fluoro-.beta.,5-dihydroxy-N-methyl-Benzene ethanamine	0.005
3-Oxobutanoicacidmethylester	0.021
4-(2-Amino-1-hydroxypropyl)phenol	0.007
4-Hydroxy-.alpha.-[(methylamino)methyl]-Benzenemethanol	0.005
6-Bromo-2-Dimethylaminomethyl-5-Methoxy-1- Methyl-1 h-Indole-3-CarboxylicAcidEthyl-ester	0.002
6-Deoxy-3-C-methyl-2-O-methyl-L-Talose	0.007
9-Hexacosene	0.009
Acetylurea	0.001
Actinobolin	0.004
Alpha.-(1-aminoethyl)-m-hydroxy-, (-)-Benzyl alcohol	0.001
Bis(2-ethylhexyl) phthalate	0.294
Cis-Aconitic anhydride	0.015
Citraconic acid	0.009
Citraconic anhydride	0.271
Clovan-2.beta.,9.beta.-diol	0.049
Crotonyl chloride	0.113
Cyanoacetylurea	0.001
Cycloeicosane	0.058
Decane	0.010
dl-Mevalonic acid lactone	0.022
Dl-Phenylephrine	0.002
Dotriacontane	0.027
E-14-Hexadecenal	0.030
Heptafluorobutanoic acid heptadecyl ester	0.057
Heptafluorobutanoic acid, 4-hexadecyl ester	0.022
Kojic acid	98.551
Malonic acid, acetyl-, dimethyl ester	0.073
N,N,N'-Trimethylurea	0.003
n-Hexadecanoic acid	0.167
n-Octadecane	0.032
Octadecanoic acid	0.035
Octadecanoic acid, 1,2,3-propanetriyl ester	0.005
Oxaluric acid	0.001
Pyrocitric acid	0.001
Tetracosane	0.034
Trans-Limonene Oxide	0.011

non-glandular (non-secretory). Non-glandular hairs were sparsely distributed, unicellular (simple), long, and pointed. This species was determined by a decreased trichome density, particularly in the long unicellular hairs (Almutawa and Roeland 2022). Combretaceous hairs were recognized by Stace (2007). The capitate-multicellular or circular-unicellular head of the glandular type was present, with a short and unicellular stalk. It is well-recognized that these trichomes

serve defensive functions (Wagner 1991). The authors here investigated some of the non- and glandular hair forms seen in the Combretaceae family, as described by Stace (1969, 2007) and Tilney (2002).

In this research, *C. erectus* had amphistomatal leaves. The stomata were also discovered by Keating (1984) on the adaxial and abaxial leaf surfaces. *C. lancifolius*, a varied species, possesses amphistomatous leaves (Redha et al. 2011 and Al-Edany and Al-Rubaie 2012). Stomata in this study were huge, measuring 37.5 × 25.0 µm, larger stomata in mangrove leaves were found to be more capable of adjusting to challenging environmental factors like salinity, according to Sternberg and Manganiello (2014). The stoma pore was observed to be narrow and short. The decrease in stomata opening was interpreted by Tomlinson (2016). He discussed that the elaboration of cuticle extension over the pore leads to decreasing pore size. That represents adaptive behavior in mangrove leaves.

Pollen grains in this study were monads, small, isopolar, and 6-heterocolpate. Some sexinous protrusions at the colpi borders formed a bridge. Namjoyan et al. (2020) discovered the same polarity and aperture type outcomes in *C. erectus* grains, with a bridge established through its endoaperture. Our results reached what they were finding. Erdtman (1952) indicated that heterocolpate pollen grains are detected in some species of the family Combretaceae. Other Myrtales families have also been found to have heterocolpate grains (Dahlgren and Thorne 1984). However, Stace (2007) mentioned this crucial trait, which helped little in understanding the generic relationships in the Combretaceae family.

The main anatomical structure of the stem and leaf of the buttonwood plant was like that of most dicots. Our observations agree with El-Mahrouk et al. (2010), who described the internal stem and leaf structure. Here, a normal-thickened cuticle layer covered both epidermal cells in the stem and leaf sections of C. erectus. This layer covered epidermal cells and introduced a defense against physiological and/or metabolic problems (Korndörfe 2006). The cuticle thickness can also reflect the solar rays' incident on the leaf. However, this structure was insignificant against the radiation because the leaf cuticle reflects only a small part of the incident radiation (Valeriano 2003).

Most parenchyma cells in our *C. erectus* stem and leaf anatomical structures were idioblasts. Idioblastic cells like oil, mucilage, crystalliferous, and tannin cells were found to occur in mangrove leaves (Tomlinson 2016). Idioblasts were defined as those cells that markedly differ in form, size, or content from neighboring cells (Castro and Demarco 2008). In this study, *C. erectus* had idioblasts of many crytalliferous druse-shaped cells. Fahn and Cutler (1992) revealed that the druses contributed to the light reflection and guiding inside the leaf. Moreover, often, druses optimize the photosynthetic performance.

Here, phenolic chemicals are present in the *C. erectus* stem and leaf. Different tissues, including the epidermis, hypodermis, cortex, palisade, and mesophyll, contained them in their cells and vacuoles. Different genera were reported to have these substances in their vacuoles (Alves 2006). In the ground tissue of stems of other families like Apocynaceae, Crassulaceae, Cyperaceae, etc., idioblasts secreting phenolic compounds were observed (Castro and Demarco 2008). In the leaves of other mangroves, such as *Laguncularia racemosa*, Lucena et al. (2011) found the phenolic compounds accumulating in the palisade cells.

The species of endophytes found in the interior tissues of *C. erectus* was *Aspergillus flavus*. Light microscopy techniques were used on stem and leaf sections to observe it. Using such microscopy tools by earlier authors (Salgado et al. 2007, Bernardi-Wenzel et al. 2010, and Verma et al. 2012) helped characterize the diversity of endofungal species.

In medicine, natural compounds are particularly important in the fight against many infections. According to Khalil et al. (2020), *C. erectus* is one of the species used to cure various illnesses, including fever, diabetes, catarrh, cancer, diarrhea, and others. Hussein (2016) examined the antibacterial effects of the plant's leaves on the bacteria *Enterobacter*, *Streptococcus*, *E. coli*, and *S. aurous*. In this study, several compounds were determined in *C. erectus* extracts and reported to have antimicrobial efficiency.

In our results, gallic acid, quercetin, rutin, rosmarinic acid, kaempferol, quercetin, sinapic, and apigenin were observed in the extracts of *C. erectus*. Gallic acid was demonstrated by Rajamanickam et al. (2019) to be effective against the pathogens *Mannheimia hemolytica* and *Pasteurella multocida*. Oliveiraa et al. (2016) demonstrated that quercetin and rutin were effective antifungal drugs when coupled with amphotericin B, allowing for a reduction in the amphotericin dose while increasing antifungal efficacy and minimizing side effects. Rosmarinic acid demonstrated antifungal activity against 11 *Candida* strains, according to Ivanov et al. (2022). Although rosmarinic acid did not bind to ergosterol, it had antifungal effects such as decreased mitochondrial activity, changed membrane integrity, and mildly suppressed protease synthesis. Antibiofilm activities include reducing exopolysaccharide synthesis, eradicating established biofilms, and preventing *Candida* adhesion. Rocha et al. (2019) reported that kaempferol and quercetin decreased ($P < 0.05$) the biomass and metabolic activity of growing biofilms of the *C. parapsilosis* complex. Parvu et al. (2015) reported that sinapic acid 0.660 $\mu g ml^{-1}$ was present in the extract of *Hederahelix* L., which showed antifungal properties against *A. niger*, *B. cinerea, S. sclerotiorum*, *F. oxysporum* f. sp. *tulipae,* and *P. gladioli*.

Lee et al. (2018) concluded that apigenin, extracted from the *Aster yomena* plant, acted as an antifungal agent

by disrupting cell membranes, inducing cell shrinkage, and disrupting membranes' ability to maintain osmotic balance. Additionally, apigenin's suppression of *C. albicans* biofilm formation may result in additional membrane alterations.

Protocatechuic acid, catechin, and syringic acid were detected in this study. Nguyen et al. (2015) have shown Protocatechuic acid and syringic acid to have antifungal action against *B. cinerea* and *Rhizoctonia solani*. To suppress any apparent mycelial growth in both *B. cinerea* and *R. solani*, PCA was shown to have a minimum inhibitory dosage of 64 mg ml^{-1}. Most *B. cinerea* conidia were injured, had altered shape, or failed to germinate after 50 and 100 mg ml^{-1} treatment. Syringic acid was shown to be the most fungitoxic compound: 0.5 mg/ml fully killed *Ganoderma boninense*, while 1.0 mg/ml only reduced the growth of the pathogen. Kumar et al. investigated catechin derivatives' antimicrobial properties (2015). For both gram-negative and gram-positive bacteria, it demonstrated excellent antibacterial action.

Based on this research, we found that endophytic fungi isolated from medicinal plants could produce natural products. We have determined kojic acid with the highest value of 98.551% and other bioactive compounds from endophytic fungi *A. flavus* isolated from *C. erectus*. *Aspergillus* species are commonly known to produce kojic acid with other metabolites (Bentley 2006). It is noted that this strain of *A. flavus* produces only kojic acid, aflatoxins and other common metabolites of *Aspergillus*, such as cylopiazonic acid, which were not detected in a study by Ola et al. (2019).

This study determined 1,2-benzenedicarboxylic acid, bis(2-ethylhexyl) ester, and 9-hexacosene in the crud extract of *A. flavus*. Kavitha et al. (2010) suggested that 1,2-benzenedicarboxylic acid, butyl 2-ethylhexyl ester play a key role in antimicrobial activity. 9-hexacosene (alpha-olefin) was analyzed from the two major compounds achieved from *Jatropha zeyheri* Sond. roots, which showed antimicrobial effects (Mongalo et al. 2019).

Actinobolin was recorded at 0.004% in this study. Actinobolin was evaluated by Armstrong and Hunt (1972) as an inhibitory agent against pure bacterial cultures: *Bacteroides melaninogenicus*, *Fusobacterium fusiforme*, *Leptotrichia buccalis*, and *Veillonella parvula*. These observations suggest that actinobolin may be effective in treating periodontal disease.

Bis(2-ethylhexyl) phthalate and decane were recorded in this study with 0.294 and 0.010%, respectively. Di-(2-Ethylhexyl) Phthalate was extracted from *Aspergillus awamori and* exhibited activity against the *Candida albicans* fungus and the Gram-positive bacteria *Sarcinalutea. DEHP* also showed cytotoxic activity against some carcinoma cell lines, as reported by Lotfy et al. (2018). Decane was extracted from the essential oil of *Artemisia aucheri* seed and showed activity against *Escherichia coli, Staphylococcus aureus*, and *Listeria monocytogenes,* as Asghari et al. (2012) suggested.

Extract of *Lasiodiplodia pseudotheobromae* showed antibacterial activity and contained bioactive components like dl-Mevalonic acid lactone and methyl (Chaithra et al. 2020); this result agreed with our study, which indicated that crude extract *of A. flavus* showed dl-Mevalonic acid lactone at 0.022%.

Dl-Phenylephrine, dotriacontane, and E-14-Hexadecenal were determined to be 0.002, 0.027, and 0.030% in the crude extract of *A. flavus*. The different concentrations of phenylephrine exhibited antibacterial activity against bacteria such as *Klebsiella pneumoniae* and *Staphylococcus aureus,* as indicated by Zin et al. (2019). Asong et al. (2019) found that petroleum ether and 50% methanol extracts from four medicinal plants showed antimicrobial activity against six microbes: *Bacillus cereus, Shigella flexneri, Candida glabrata, Candida krusei, Trichophyton rubrum,* and *Trichophyton tonsurans,* using the microdilution test. GC–MS analysis revealed the presence of dotriacontane as a bioactive component. After being analyzed with GC–MS, Abraham et al. (2018) revealed that crude extracts of *Pseudarthria viscida* and its endophytes have E-14-Hexadecenaland (with). Most of the compounds in the extracts were identified as possessing therapeutic properties.

N-Octadecane and tetracosane were represented by 0.032 and 0.034% in the crude extract of *A. flavus,* respectively. Based on the analysis of GCSP, n-octadecane (30.5%) was detected in the bulb oil of *Allium nigrum* L. that exhibited antimicrobial activity, especially against *Enterococcus faecalis* and *Staphylococcus aureus* (Rouis-Soussi et al. 2014). *Allium tripedale* extract had a considerable inhibitory effect against various *Candida* species, and among the major components of the extract was tetracosane.

In conclusion, this study documented the morphological characteristics and internal anatomy of the stems and leaves of *Conocarpus erectus* L. and introduced palynological information. The morpho-anatomical attributes considered the structural arrangement of plant tissues, phytochemicals, and endophytes. The antifungal activity of plant extracts and their endophytes resulted from active metabolites such as kojic acid, gallic acid, rutin, and rosmarinic acid.

Funding Open access funding provided by The Science, Technology & Innovation Funding Authority (STDF) in cooperation with The Egyptian Knowledge Bank (EKB).

Data availability Data were available in the manuscript and at NCBI.

Declarations

Ethical approval The Institute Ethics Committee approved the study protocol. Approval for fungal isolates in this study was granted by theResearch Ethics Committee of Faculty of Science, South Valley University, Egypt (No.: 001/11/22).

Conflict of interest None.

References

Abdel-Hameed ES, Bazaid SA, Shohayeb MS, El-Sayed MM, El-Wakil EA (2012) Phytochemical studies and evaluation of antioxidant, anticancer and antimicrobial properties of *Conocarpus erectus* L. growing in Taif, Saudi Arabia. Euro J Med Plants 2:93–112

Abdel-Hameed ESS, Bazaid SA, Sabra ANA (2013) Protective effect of *Conocarpus erectus* extracts on CCl4-induced chronic liver injury in mice. Glob J Pharmacol 7:52–60. https://doi.org/10.5829/idosi.gjp.2013.7.1.7188

Abraham D, Nair B, Mallikarjunaswamy GE (2018) Antimicrobial and GCMS Analysis of chloroform extract of *PseudarthriaViscida* (L.) Wight and Arn. and associated major fungal endophyte. Int J Adv Res 7(1):105–113. https://doi.org/10.21474/IJAR01/8302

Afifi HS, Al Marzooqi HM, Tabbaa MJ, Arran AA (2021) Phytochemicals of Conocarpus spp. as a natural and safe source of phenolic compounds and antioxidants. Molecules 26:1069. https://doi.org/10.3390/molecules26041069

Al-Edany TY, Al-Rubaie EMA (2012) Morphological and Anatomical Study of *Conocarpus lancifolius* Engl. (Combretaceae) in Iraq. Basrah J Agric Sci 25(1):39–49

Ali AT (2018) The Biological activity of *Conocarpus erectus* extracts and their application as cytotoxic agents. Fac Biotechnol, October Univ for Mod Sci and Arts, Research Project [RS401]

Almutawa AA, Roeland S (2022) Comparative Study of *Conocarpus erectus* and *Phoenix dactylifera* as plant biomonitors of particulate matter pollution in Kuwait over three land use classes. Atmo Clim Sci 12:189–234

Alves GM (2006) Anatomia foliar de leguminosas arbóreas de cerrado com ênfase nas estruturas secretoras MS Thesis. Universida de Estadual de Campinas, Campinas, São Paulo, Brazil

Al-Wabel MI, Usman AR, El-Naggar AH, Aly AA, Ibrahim HM, Elmaghraby S, Al Omran A (2015) *Conocarpus* biochar as a soil amendment for reducing heavy metal availability and uptake by maize plants. Saudi J Biol Sci 22:503–511

Arachevaleta M, Bacon C, Hoveland C, Radcliffe D (1989) Effect of the tall fescue endophyte on plant response to environmental stress. Agronomy J 81(1):83–90. https://doi.org/10.2134/agronj1989.00021962008100010015x

Armstrong JRPJ, Hunt DE (1972) In vitro evaluation of Actinobolin as an antibiotic for the treatment of periodontal disease. App Microbiol 23(1):88–90. https://doi.org/10.1128/am.23.1.88-90.1972

Asghari G, Jalali M, Sadoughi E (2012) Antimicrobial activity and chemical composition of essential oil from the seeds *of Artemisia aucheri* Boiss. Jundishapur J Nat Pharm Prod 7(1):11–15. https://doi.org/10.5812/kowsar.17357780.3530

Asong JA, Amoo SO, McGaw LJ, Nkadimeng SM, Aremu AO, Otang-Mbeng W (2019) Antimicrobial Activity, antioxidant potential, cytotoxicity and phytochemical profiling of four plants locally used against skin diseases. Plants 8:350. https://doi.org/10.3390/2Fplants8090350

Aziz MA, Khan AH, Adnan M, Ullah H (2018) Traditional uses of medicinal plants used by Indigenous communities for veterinary practices at Bajaur Agency, Pakistan. J Ethnobiol Ethnomed 14:11. https://doi.org/10.1186/s13002-018-0212-0

Bailey L (1976) Hortus Third: A concise dictionary of plant cultivated in US and Canada. Rep. No. 306. Macmillan publishing Co. Inc

Bashir M, Uzair M, Chaudhry BA (2015) A review of phytochemical and biological studies on *Conocarpus erectus* (Combretaceae). Pak J Pharam Res 1(1):1–8

Bayoub K, Baibai T, Mountassif D, Retmane A, Soukri A (2010) Antibacterial activities of the crude ethanol extracts of medicinal plants against *Listeria monocytogenes* and some other pathogenic strains. Afr J Biotechnol 9(27):4251–4258

Bentley R (2006) From miso, saké and shoyu to cosmetics: a century of science for kojic acid. Nat Prod Rep 23:1046–1062. https://doi.org/10.1039/b603758p

Bernardi-Wenzel J, Garcia A, Filho CJR, Prioli AJ, Pamphile JA (2010) Evaluation of foliar fungal endophyte diversity and colonization of medicinal plant *Luehea divaricata* (Martius et 75–384 Zuccarini). Biol Res 43:375–384

Castro MM, Demarco D (2008) Phenolic compounds produced by secretory structures in plants: a brief review. Nat Prod Communications 3(8):1273–1284. https://doi.org/10.1177/1934578X0800300809

Chaithra M, Vanitha S, Ramanathan A, Jegadeeshwari V, Rajesh V, Hegde V, Apshara E (2020) Profiling secondary metabolites of Cocoa (*Theobroma cacao* L.) Endophytic fungi *Lasiodiplodia pseudotheobromae* PAK-7 and *Lasiodiplodia theobromae* TN-R-3 and their antimicrobial activities. Curr J Appl Sci Technol 39:47–56. https://doi.org/10.9734/cjast/2020/v39i230496

Clarke J (1960) Preparation of leaf epidermis for topographic study. Stain Tech 35(1):35–39. https://doi.org/10.3109/10520296009114713

Dahlgren R, Thorne RF (1984) The order Myrtales: circumscription, variation, and relationships. Ann Miss Bot Gard 71(3):633–699. https://doi.org/10.2307/2399158

DÍaz-Castelazo C, Rico-Gray V, Ortega F, Ángeles G (2005) Morphological and secretory characterization of extrafloral nectaries in plants of Coastal Veracruz, Mexico. Ann Bot 96:1175-1189.https://doi.org/10.1093/aob/mci270

Elias TS (1983) Extrafloral Nectaries: Their Structure and Distribution. In: Bentley B, Elias T (eds) The Biology of Nectaries. Columbia University Press, New York, pp 174–203

El-Mahrouk ME, El-Nady MF, Hegazi MA (2010) Effect of diluted seawater irrigation and exogenous proline treatment on growth, chemical composition and anatomical characteristics of *Conocarpus erectus* L. J Agric Research Kafrelsheikh Univ 36(4):420–446

Erdtman G (1952) Pollen morphology and plant taxonomy, Angiosperms. Almqvist and wiksell, Stockholm, pp 553

Fahn A, Cutler D (1992) Xerophytes. Gebruder Borntraeger, Berlin

Gilman EF, Watson DG (1993) Conocarpus erectus. Forest Service, Dept Agric 179:1–3

Hussein RA (2016) Evaluation antioxidant and antibacterial activities of n-Butanol fraction of *Conocarpus erectus* L. leaves extract. Int J Pharm Med Res 4:394–400

Ivanov M, Kostić M, Stojković D, Soković M (2022) Rosmarinic acid–Modes of antimicrobial and antibiofilm activities of common plant polyphenol. South Afr J Bot 146:521–527. https://doi.org/10.1016/j.sajb.2021.11.050

Ivanova E, Pancevska NA, Kungulovski Dz (2013) Antimicrobial activities of laboratory-produced essential oil solutions against five

selected fungal strains. Proc Natural Sci Maticasrpska (Novi Sad Serbia) 124:171–185. https://doi.org/10.2298/ZMSPN1324171I
Johansen DA (1940) Plant Micro-technique. McGraw- Hill New-York, pp. 523
Kamel M, El-Hadidy A, Thabet S, Hussein NRA (2019) A Palynological review for some species of family boraginaceae juss. Ann Res Rev Biol 30(3):1–16. https://doi.org/10.9734/ARRB/2018/46408
Kavitha A, Prabhakar P, Narasimhulu M, Vijayalakshmi M, Venkateswarlu Y, Rao KV et al (2010) Isolation, characterization, and biological evaluation of bioactive metabolites from Nocardia levis MK-VL_113. Microbiol Res 165:199–210. https://doi.org/10.1016/j.micres.2009.05.002
Keating RC (1984) Leaf histology and its contribution to relationships in the Myrtales. Ann Miss Bot Garden 71(3):801–823. https://doi.org/10.2307/2399163
Khalil R, Ali Q, Hafeez MM, Malik A (2020) Phytochemical activities of *Conocarpus erectus*: An overview. Biol Clin Sci Res J https://doi.org/10.54112/bcsrj.v2020i1.8
Kim KH, Tsao R, Yang R, Cui SW (2006) Phenolic acid profiles and antioxidant activities of wheat bran extracts and the effect of hydrolysis conditions. Food Chemist 95:466–473. https://doi.org/10.1016/j.foodchem.2005.01.032
Koche D, Shirsat R, Kawale M (2016) An overview of major classes of phytochemicals: their types and role in disease prevention. Hislopia J 9(1–2):1–11
Koptur S (1992) Plants with extrafloral nectatries and ants in everglades habitats. Florida Entomologist 75:39–50
Korndörfe AP (2006) Aimportância do silícionasrelações entre herbívoros e *Davillaelliptica* (Dilleniaceae) St. Hil no cerrado. Dissertação de Mestrado, Curso de PósGraduaçãoem Conservação de Recursos Naturais. UFU, Uberlândia, MG
Kumar D, Poornima M, Kushwaha RN, Won T, Ahn C, Kumar CG, Jang K, Shin D (2015) Antimicrobial and docking studies of (-)-catechin derivatives. J Korean Soc Appl Biol Chem 58(4):581–585. https://doi.org/10.1007/s13765-015-0079-x
Lee H, Eun-Rhan Woo E, Lee DG (2018) Apigenin induces cell shrinkage in *Candida albicans* by membrane perturbation. FEMS Yeast Res18(1). https://doi.org/10.1093/femsyr/foy003
Lotfy MM, Hassan HM, Hett MH, El-Gendy AO, Mohammed R (2018) Di-(2-ethylhexyl) Phthalate, a major bioactive metabolite with antimicrobial and cytotoxic activity isolated from River Nile derived fungus *Aspergillus awamori*. Beni-Suef Univ J Basic App Sci 7:263–269. https://doi.org/10.1016/j.bjbas.2018.02.002
Lucena I, Maciel VE, Silva JB, Galvíncio JD, Pimentel RM (2011) Leaf structure of mangrove species to understand the spectral responses. J Hyperspectral Remote Sensing 2:19–31
Mongalo NI, Soyingbe OS, Makhafola TJ (2019) Antimicrobial, cytotoxicity, anticancer and antioxidant activities of *Jatropha zeyheri* Sond. roots (Euphorbiaceae). Asian Pacific J Trop Biomedicine 9(7):307–314
Moubasher AH (1993) Soil fungi in Qatar and other Arab countries. Sci Appl Res Centre, Univ of Qatar, Doha, Qatar 566. https://doi.org/10.1007/BF02861455
Namjoyan F, Farasat M, Kiabi S, Ramezani Z, Mousavi H (2020) Structural and ultra-structural analysis of *Conocarpus erectus* pollen grains before and after dust storms. Grana 59(2–3):226–237. https://doi.org/10.1080/00173134.2019.1689290
Nascimento D, De Souza IA, Barbosa MO, Santana MAN, Júnior DFP, Lira EC, Vieira JRC (2016) Phytochemical screening and acute toxicity of aqueous extract of leaves of *Conocarpus erectus* linnaeus in Swiss Albino Mice. Ann Acad Bras Ciênc 88(3) Rio de Janeiro Sept. Epub Aug 04. https://doi.org/10.1590/0001-3765201620150391
Nelson G (1996) The shrubs and woody vines of Florida. Pineapple Press Inc, Sarasota, FL., p 391
Nguyen XH, Naing KW, Lee YS, Moon JH, Kim Lee JH, KY, (2015) Isolation and characteristics of protocatechuic acid from Paenibacilluselgii HOA73 against Botrytis cinerea on strawberry fruits. J Basic Microbiol 55:625–634. https://doi.org/10.1002/jobm.201400041
Ola ARB, Metboki G, Lay CS, Sugi Y, De Rozari P, Darmakusuma D, Hakim EH (2019) Single production of Kojic acid by Aspergillus flavus and the revision of Flufuran. Molecules 24:4200. https://doi.org/10.3390/molecules24224200
Oliveiraa VM, Carraroa E, Aulerb ME, Khalil NM (2016) Quercetin and rutin as potential agents antifungal against Cryptococcus spp. Braz J Biol 76(4):1029–1034. https://doi.org/10.1590/1519-6984.07415
Parvu M, Vlase L, Pârvu AE, Rosca-Casian O, Gheldiu A-M, Pârvu O (2015) Phenolic compounds and antifungal activity of *Hedera helix* L. (Ivy) flowers and fruits. Not Bot Horti Agrobo 43(1):53-58. https://doi.org/10.15835/nbha4319644
Popp M, Uttge UL, Cram WJ, Diaz M, Griffiths H, Lee HJS, Medina E, Schäfer C, Stimmel KH, Thonke B (1989) Water relations and gas exchange of mangroves. New Phytol 111:293–307
Punt W, Hoen PP, Blackmore S, Nilson S, Le Thomas A (2007) Glossary of pollen and spore terminology. Rev Palae Palynol 143:1–81. https://doi.org/10.1016/j.revpalbo.2006.06.008
Rajamanickam K, Yang J, Sakharkar MK (2019) Gallic acid potentiates the antimicrobial activity of Tulathromycin against two key bovine respiratory disease (BRD) causing-pathogens. 9:1486. https://doi.org/10.3389/fphar.2018.01486
Raza MA, Anwar F, Shahwar D, Majeed A, Mumtaz MW, Danish M, Nazar MF, Perveen I, Khan SUD (2016) Antioxidant and antiacetylcholine esterase potential of aerial parts of *Conocarpus erectus*, *Ficus variegata* and *Ficus maclellandii*. Pak J Pharm Sci 29(2):489–495
Raza SA, Chaudhary AR, Mumtaz MW, Ghaffar A, Adnan A, Waheed A (2018) Antihyperglycemic effect of *Conocarpus erectus* leaf extract in alloxan-induced diabeticmice. Pak J Pharma Sci 31(2):637–642
Redha A, Al-Mansour N, Suleman P, Afzal M, Al-Hasan R (2011) Leaf traits and histochemistry of trichomes of *Conocarpus lancifolius* a combretaceae in semi-arid conditions. Am J Pl Sci 2:165–174. https://doi.org/10.4236/ajps.2011.22018
Rocha MFG, Sales JA, da Rocha MG, Galdino LM, de Aguiar L, Pereira-Neto W, Cordeiro R, Castelo-Branco D, Sidrim JJ, Brilhante RSN (2019) Antifungal effects of the flavonoids kaempferol and quercetin: apossible alternative for the control of fungal biofilms. Biofoul 35(3):320–328. https://doi.org/10.1080/08927014.2019.1604948
Rosa Galdino Bandeira A (2003) Estudo Fitoquímico e Atividade Biológica de *Conocarpus erectus* L. (Manguebotão). https://repositorio.ufpe.br/handle/123456789/1329
Rossman AY, Tulloss RE, O'Dell TE, Thorn RG (1998) Protocols for an all-taxa biodiversity inventory of fungi in a Costa Rican conservation area.Parkway Publications, Inc., Boone, North Carolina 163. https://doi.org/10.2307/3761287
Rouis-Soussi LS, El Ayeb-Zakhama A, Mahjoub A, Flamini G, Ben Jannet H, Harzallah-Skhiri F (2014) Chemical composition and antibacterial activity of essential oils from the Tunisian *Allium Nigrum* L. Excli J 13:526–535
Sabi-ur-rehman AF, Ur Rehman S, Ur Rahman T, Mehmood A, Gohar A, Samad Abdul (2019) A review on botanical, phytochemical and pharmacological reports of *Conocarpus erectus*. Pak J Agric Res 32(1):212–217. https://doi.org/10.17582/journal.pjar/2019/32.1.212.217
Saeedi M, Eslamifar M, Khezri K (2019) Kojic acid applications in cosmetic and pharmaceutical preparations. BiomedPharm 110:582–593. https://doi.org/10.1016/j.biopha.2018.12.006

Salgado C, Cepero MC, Realpe E, Restrepo S (2007) Histological analyses of the fungal endophytes in *Rosa hybrida*. Rev Iberoam Micol 24:323–324

Santos D, De-Almeida VS, De Araujo DRC, Harand W, Soares AKDA, Moreira LR, De Lorena VMB, Magalhães LPM, Ximenes RM, DeSena KXDFR (2018) Evaluation of cytotoxic, immunomodulatory and antibacterial activitiesof aqueous extract from leaves of *Conocarpus erectus* Linnaeus (Combretaceae). J Pharma Pharmacol 70:1092–1101. https://doi.org/10.1111/jphp.12930

Schoener TW (1988) Leaf damage in island buttonwood, *Conocarpus erectus*: correlations with pubescence, island area, isolation and the distribution of major carnivores. Oikos 253–266. https://doi.org/10.2307/3566071

Shohayeb M, Abdel-Hameed E, Bazaid S (2013) Antimicrobial activity of tannins and extracts of different parts of *Conocarpus erectus* L. Int J Pharm Bio Sci 3(2):544–553

Silva MRO, Almeida AC, Arruda FVF, Gusmao N (2011) Endophytic fungi from Brazillian mangrove plant *Laguncularia racemosa* (L.) Gaertn. (Combretaceae): their antimicrobial potential. Sci Against Microbpathog: Commun Current Res Technolo Adv 2:1260–1266

Stace CA (1969) The significance of the leaf epidermis in the taxonomy of the Combretaceae III. The genus combretum in America. Brittonia 21(2):130–143

Stace CA (2007) Combretaceae. In: Kubitzki K (ed.) The Families and Genera of Vascular Plants, vol. IX. Springer-Verlag Berlin Heidelberg

Stearn WT (1983) Botanical Latin, 3rd edn. David & Charles Ltd., Great Britan

Sternberg LSL, Manganiello LM (2014) Stomatal pore size and density in mangrove leaves and artificial leaves: Effects on leaf water isotopic enrichment during transpiration. Func Pl Biol 41:648–658. https://doi.org/10.1071/FP13235

Tan RX, Zou WX (2001) Endophytes: a rich source of functional metabolites. Nat Prod Rep 18(4):448–459. https://doi.org/10.1039/B100918O

Tilney PM (2002) A contribution to the leaf and young stem anatomy of the Combretaceae. Bot J Linn Soc 138:163–196

Tomlinson PB (2016) The botany of mangroves, 2nd edn. Cambridge University Press, Cambridge

Valeriano MM (2003) Reflectância espectral de culturas agrícolas anuais (I): espectrorra diometria. Espaço Geografia 6(1):1–22

Verma VC, Singh SK, Kharwar RN (2012) Histological investigation of fungalendophytes in healthy tissues of *Azadirachta indica* A. Juss. Kasetsart J (Nat Sci) 46(2):229–237

Wagner GT (1991) Secreting glandular trichomes: more than just hairs. Pl Physiol 96(3):675–679

Wen J, Okyere SK, Wang S, Wang J, Xie L, Ran Y, Hu Y (2022) Endophytic fungi: an effective alternative source of plant-derived bioactive compounds for pharmacological. Stud J Fungi 8:205. https://doi.org/10.3390/jof8020205

Wilson D (1995) Endophyte: the evolution of a term, and clarification of its use and definition. Oikos 73(2):274–276. https://doi.org/10.2307/3545919

Zin T, Sivakumar J, Sundaram CS, Rao US (2019) In silico analysis of the phenylephrine from the sand crab (*Emerita asiatica*) for its antimicrobial activities. Res J Pharm Tech 12(5):2145–2152